Optica Applicata, Vol. XLIX, No. 3, 2019
DOI: 10.5277/oa190309

Linear and nonlinear TM polarized surface waves in anisotropic metamaterials

MUNAZZA ZULFIQAR ALI

Physics Department, Punjab University, Lahore 545900, Pakistan; munazzazulfiqar@yahoo.com

The metamaterial with an effective permeability and/or permittivity tensor having elements of different magnitudes and signs is termed as the anisotropic metamaterial. The hyperbolic metamaterial may be considered as a subclass of the anisotropic metamaterial. The dispersion relation for the transverse magnetic surface waves at the interface between a nonlinear dielectric material and an anisotropic metamaterial is derived using the parallel uniaxial approximation of the permittivity tensor. This dispersion relations can be linearized by taking the nonlinear coefficient to be zero. Dispersion curves are plotted for both the linear and the nonlinear cases and are analyzed and compared in different frequency regions.

Keywords: anisotropic metamaterials, surface plasmons, nonlinear waves.

1. Introduction

Metamaterials are artificially engineered subwavelength composites offering a wide range of material parameter choices that do not occur in nature [1]. Their conceptual and subsequent experimental development in the recent past has inspired the scientists to think of novel possibilities in science and technology. There are different types of metamaterials, including the negative refractive-index metamaterials, the chiral metamaterials, the hyperbolic and the anisotropic metamaterials *etc*. [2–5]. The anisotropic metamaterials are characterized by the effective permittivity and/or permeability tensors with components different in magnitudes and signs [5–13]. These are under considerable theoretical and experimental investigations these days due to their potential applications such as antireflectors [6], negative refraction and superlensing effects [7–10] optical fibre guiding structures [11], invisibility cloaks and many others [12]. When the permeability is isotropic and the effective permittivity tensor is uniaxial, then its components are either parallel or perpendicular to the optical axis. The signs of these parallel and perpendicular components may or may not be the same. If these are of opposite signs, we have the hyperbolic metamaterials. The nomenclature comes from the hyperbolic isofrequency curves of these metamaterials. These hyperbolic metamaterials are generally subwavelength metal-dielectric multilayer structures or graphene

based nanostructures. These are under intensive investigations these days because of their astonishing properties which have got applications in the field of negative refraction, subwavelength imaging and holography [14–21]. An important application of the hyperbolic metamaterials is in the field of surface waves. Surface waves are important because of their sensitivity and field localization that lead to immense applications. There have been a lot of studies on the nature and character of surface waves in hyperbolic metamaterial and in anisotropic metamaterial in general [22–24]. These include the very recent study of surface plasmon-polaritons at the interface of two different anisotropic metamaterials formed by stacking metal-dielectric layers [22]. After the pioneering work on the Dyakonov surface waves [25], their different types and forms have also been studied and analyzed at the interfaces between uniaxial metamaterial and dielectric material [26–30]. The investigations into the formation and characteristics of surface waves at the interface of an anisotropic hyperbolic metamaterial and a doped semiconductor material have also been carried out [31]. The existence regimes of various types of surface waves at the interface of a dielectric and an anisotropic metamaterial have also been explored [32]. Generally, the inclusion of nonlinearity leads to the formation regions of surface waves for frequencies where linear surface waves do not exist. The nonlinear surface waves are also used to engineer the group velocity and to change the handedness (*i.e.* from left handedness to right handedness and *vice versa*) [33]. Here we consider the interface between a dielectric and an anisotropic metamaterial. The anisotropic metamaterial under consideration is merely a subwavelength metal-dielectric multilayer structure whose filling factor decides its anisotropic or hyperbolic behavior in a particular frequency region. For a given choice of the filling factor, the dispersive behavior depends on the frequency region. Here, the problem is set in a general way and the anisotropic metamaterial is treated on the frequency scale in which it shows the hyperbolic type I, type II and simple anisotropic behaviors. We investigate the existence of linear and nonlinear surface waves for the transverse magnetic (TM) polarized waves at the interface under consideration. In the case of nonlinear TM surface waves, the analytical solutions in different types of media have been discussed previously under various approximations [34–39]. Here we have applied one such approximation known as the uniaxial parallel approximation to study the formation of surface modes at the interface between a nonlinear dielectric material and an anisotropic metamaterial. This approximation is applied previously to study the nonlinear surface waves at the interfaces of linear and/or nonlinear dielectric material and a very recent study on nonlinear surface waves in photonic hypercrystals [33]. Our treatment is the general one that includes different types of anisotropic metamaterials and also studies on both linear and nonlinear cases under the uniaxial approximation. Such a treatment is not present in the literature to the best of our knowledge. The dispersion relation is derived and the corresponding curves are plotted for different parameters. Initially the nonlinear coefficient is taken to be zero and curves are plotted for the linear dispersion relation. Then the nonlinear dispersion curves are plotted and comparison is made with the linear dispersion curves in different frequency regions. The effect of material losses is considered in the end.

2. Mathematical model

Here we consider the interface at $z = 0$, between a nonlinear dielectric ($z < 0$) and an anisotropic metamaterial ($z > 0$) as shown schematically in Fig. 1. Since we are considering the surface waves propagating along the x direction, the electric and magnetic fields can be specified as

$$\mathbf{E}(\mathbf{r}, t) = \mathbf{E}(z)\exp\left[i(k_x x - \omega t)\right] \tag{1a}$$

$$\mathbf{H}(\mathbf{r}, t) = \mathbf{H}(z)\exp\left[i(k_x x - \omega t)\right] \tag{1b}$$

For the TM polarized waves in the present geometry, $E_y = H_x = H_z = 0$ and for $z < 0$, the nonlinear TM waves are characterized by the following 2×2 subtensor of electric permittivity

$$\varepsilon^{\mathrm{TM}} = \begin{bmatrix} \varepsilon_x + \alpha_{xx}|E_x|^2 + \alpha_{xz}|E_z|^2 & 0 \\ 0 & \varepsilon_z + \alpha_{zz}|E_z|^2 + \alpha_{zx}|E_x|^2 \end{bmatrix} \tag{2}$$

The above permittivity tensor can be discussed under various approximations, here we consider the parallel uniaxial approximation [37] according to which:

$$\alpha_{xx} = \alpha, \quad \alpha_{xz} = \alpha_{zx} = \alpha_{zz} = 0, \quad \varepsilon_x = \varepsilon_z = \varepsilon \tag{3}$$

The nonlinear refractive index is given as

$$n = \sqrt{\varepsilon} + n_{\mathrm{nl}}|E|^2 \tag{4}$$

and the nonlinear coefficients are related as

$$\alpha = 2\sqrt{\varepsilon}\, n_{\mathrm{nl}} \tag{5}$$

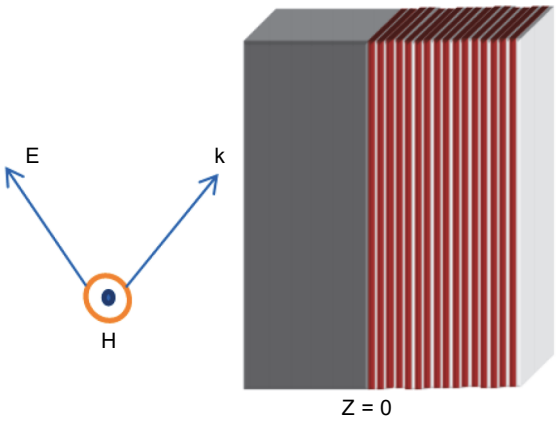

Fig. 1. Schematic diagram of the interface between the dielectric and the hyperbolic metamaterial.

It is appropriate to consider the parallel uniaxial approximation for the surface waves since it allows the nonlinearity to be effective in the transverse direction (along the x-axis in the present case). So the permittivity tensor becomes:

$$\varepsilon^{\mathrm{TM}} = \begin{bmatrix} \varepsilon + \alpha |E_x|^2 & 0 \\ 0 & \varepsilon \end{bmatrix} \tag{6}$$

Starting with Maxwell's equations:

$$\nabla \times E = -\frac{\partial B}{\partial t}, \qquad \nabla \times H = \frac{\partial D}{\partial t} \tag{7}$$

The following set of equations is obtained:

$$ik_x E_z + \frac{\partial E_x}{\partial z} = -\mu_0 i\omega H_y \tag{8a}$$

$$-\frac{\partial H_y}{\partial z} = i\omega\varepsilon_0 \left[\varepsilon + \alpha |E_x|^2\right] E_x \tag{8b}$$

$$-k_x H_y = \omega\varepsilon\varepsilon_0 E_z \tag{8c}$$

Eliminating E_z and H_y among the set of equations, we get an equation in E_x

$$\frac{\partial^2 E_x}{\partial z^2} - k_z^2 \left[1 + \frac{\alpha}{\varepsilon} |E_x|^2\right] E_x = 0 \tag{9}$$

where we have used $c^2 = 1/(\varepsilon_0\mu_0)$, and $k_z^2 = k_x^2 - k^2$, where k is the magnitude of the wave vector inside the material and k_x and k_z being its components in the indicated directions. The above equation has an analytic solution [39]

$$E_x(z) = \sqrt{\frac{2\varepsilon}{|\alpha|}}\, \mathrm{csch}\left[k_z(z_c - z)\right] \tag{10}$$

where z_c is the constant of integration to be determined by the boundary conditions. Now since:

$$\frac{\partial H_y}{\partial z} = -i\omega\varepsilon_0 \left[\varepsilon + \alpha |E_x|^2\right] E_x \tag{11}$$

Substituting E_x from (10) in the above equation and performing integration

$$H_y(z) = \frac{-i\varepsilon_0\varepsilon\omega}{k_z} \sqrt{\frac{2\varepsilon}{|\alpha|}}\, \mathrm{csch}\left[k_z(z_c - z)\right] \coth\left[k_z(z_c - z)\right] \tag{12}$$

For $z > 0$, we have an anisotropic metamaterial consisting of subwavelength layers of a metal with permittivity ε_m and layer width d_m and a dielectric material with electric

permittivity ε_d and layer width d_d. Its effective normal and tangential components are represented by ε_n and ε_t, respectively, and by using the effective medium theory they come out to be:

$$\varepsilon_t = p\varepsilon_m + (1-p)\varepsilon_d \tag{13a}$$

$$\varepsilon_n = \frac{\varepsilon_m \varepsilon_d}{p\varepsilon_d + (1-p)\varepsilon_m} \tag{13b}$$

$$p = \frac{d_m}{d_m + d_d} \tag{13c}$$

It means that the permittivity matrix in the hyperbolic metamaterial can be written as

$$\varepsilon_h = \begin{bmatrix} \varepsilon_t & 0 & 0 \\ 0 & \varepsilon_t & 0 \\ 0 & 0 & \varepsilon_n \end{bmatrix} \tag{14}$$

Again stating from Maxwell's equations for TM polarization, the tangential component of the electric field follows the equation

$$\frac{\partial^2 E_x}{\partial z^2} + \left(\frac{\omega^2}{c^2}\varepsilon_t - \frac{\varepsilon_t}{\varepsilon_n} k_x^2 \right) E_x = 0 \tag{15}$$

Since we are looking for the waves that are localized on the x-axis and decay in the z direction, so the assumed solution for the above equation is

$$E_x(z) = E_0 \exp(-\beta z) \tag{16}$$

where E_0 is the amplitude of the incident field and

$$\beta = \sqrt{\frac{\varepsilon_t}{\varepsilon_n} k_x^2 - \frac{\omega^2}{c^2}\varepsilon_t} \tag{17}$$

Since

$$\frac{\partial H_y}{\partial z} = -i\omega\varepsilon_0\varepsilon_t E_x \tag{18}$$

the tangential component of the magnetic field, *i.e.* H_y, comes out to be:

$$H_y(z) = H_0 \exp(-\beta z) \tag{19a}$$

$$H_0 = \frac{i\omega\varepsilon_0\varepsilon_t}{\beta} E_0 \tag{19b}$$

Now applying the boundary conditions, *i.e.* equating the tangential components of electric and magnetic fields at $z = 0$, from the balance of the electric field equations we get

$$z_c = \frac{1}{k_z}\operatorname{csch}^{-1}\left(\frac{E_0\sqrt{\alpha}}{\sqrt{2\varepsilon}}\right) \tag{20}$$

Balancing the magnetic fields and making substitution from the above equation, after simplifications we get

$$k_x^2\left(\frac{\varepsilon_d}{\varepsilon_n}A - \frac{\varepsilon_t}{\varepsilon_d}\right) - \frac{\omega^2}{c^2}(\varepsilon_d A - \varepsilon_t) = 0 \tag{21}$$

where

$$A = \coth^2\left\{\operatorname{csch}^{-1}\left[E_0\left(\sqrt{\frac{\alpha}{2\varepsilon_d}}\right)\right]\right\} \tag{22}$$

In the limit $\alpha \to 0$, $A \to 1$ and the relation (21) it reduces to the linear dispersion relation [31]

3. Results and discussions

Now we use Eq. (21) to investigate the various characteristics of the dispersion relation. There can be various choices for the dielectric material and the constituents of the anisotropic metamaterial. For the present computational work, the following parameters are chosen in the mid infrared frequency range: for $z < 0$, Al_2O_3 is considered to be the nonlinear dielectric with linear refractive index $n_0 = \sqrt{\varepsilon} = 1.8$ and nonlinear coefficient $n_{nl} = 2.9 \times 10^{-14}$ cm^{2}W^{-1} [40]. For $z > 0$, the anisotropic metamaterial consists of alternate nanometer sized layers of silver with permittivity $\varepsilon_m = 5 - \omega_p^2/(\omega^2 + i\omega\gamma)$, $\omega_p/2\pi \approx 2175$ THz, $\gamma/2\pi \approx 4.35$ THz and a dielectric ($Al_{0.48}In_{0.52}As$) with permittivity $\varepsilon_d = 10.23$. The material losses can be safely neglected in the present case as the damping coefficient γ is much smaller than the frequency range of interest. So, the linear and nonlinear dispersion relation curves are drawn by taking $\gamma = 0$, however the effect of material losses is considered lastly by taking the actual value of γ to plot the figure of merit (FOM) and the extinction coefficient curves of the lossy metamaterial.

First we draw the effective parameters curves of the anisotropic metamaterial. Figure 2 shows the effective transverse permittivity ε_t (blue curves) and the effective normal permittivity ε_n (red curves) as a function of dimensionless frequency ($W = \omega d/c$) for three different values of the filling factor p given in the figure captions. The whole

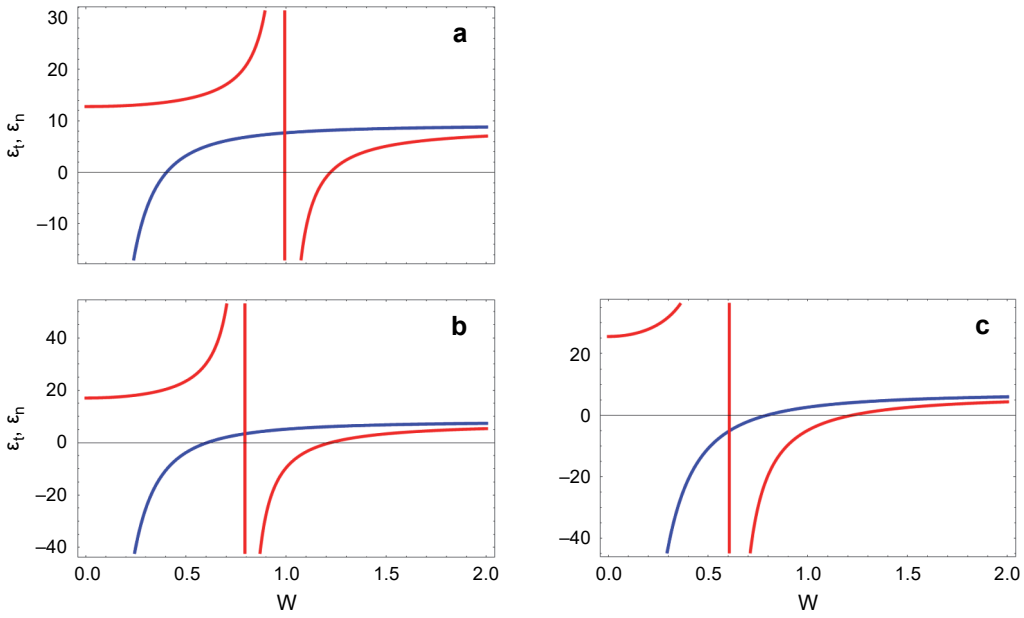

Fig. 2. The plots of the normal ε_n (red curve) and the tangential ε_t (blue curve) components of the permittivity tensor for different values of the filling factor $p = 0.2$ (**a**), $p = 0.4$ (**b**), and $p = 0.6$ (**c**).

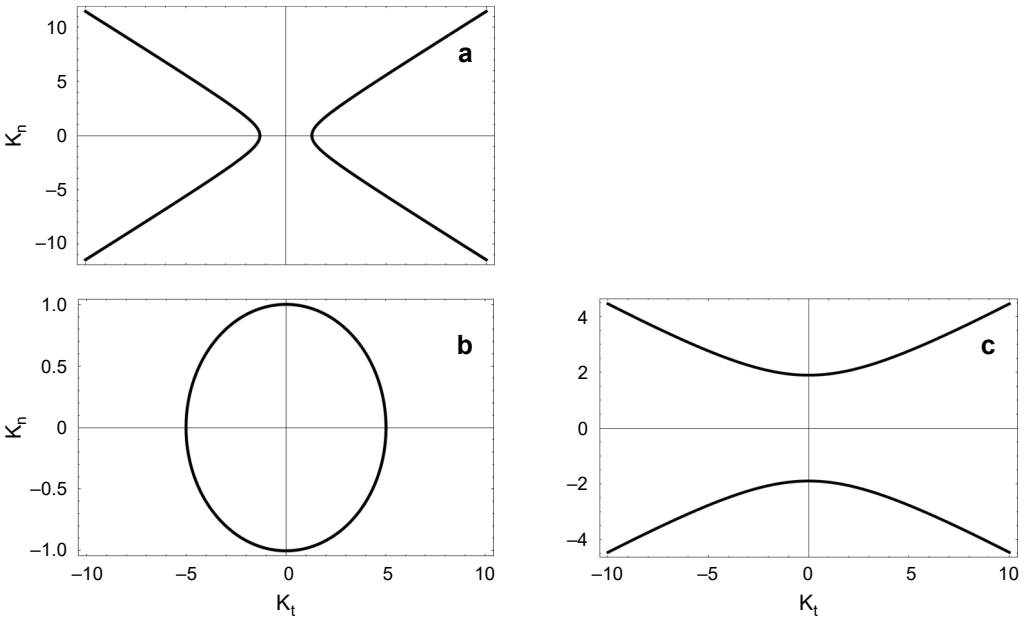

Fig. 3. The isofrequency plots of K_n *vs*. K_t corresponding to $p = 0.4$ for different values of frequencies $W = 0.3$ (**a**), $W = 0.7$ (**b**), and $W = 0.9$ (**c**).

behavior can be divided into three anisotropic regions: the frequency region with $\varepsilon_t < 0$, $\varepsilon_n > 0$ corresponds to type II hyperbolic behavior, $\varepsilon_n < 0$, $\varepsilon_t > 0$ corresponds to type I hyperbolic behavior whereas in the third anisotropic region both components of the permittivity tensor are positive but unequal in magnitude. The figures show that the three regions are dependent on the filling factor and can be engineered by changing the filling factor of the metamaterial.

Figure 3 shows the K_x *vs*. K_z ($K_x = k_x d$ and $K_z = \beta d$) plots for a particular choice of the filling factor $p = 0.4$. Figure 3 corresponds to the cases when the metamaterial behaves as anisotropic hyperbolic type II at $W = 0.3$, simple anisotropic at $W = 0.7$, and anisotropic hyperbolic type I metamaterial at $W = 0.9$.

Initially we have plotted Eq. (21) by taking the nonlinear coefficient α equal to zero. Figure 4 shows the dispersion curves of the linear surface waves for three different values

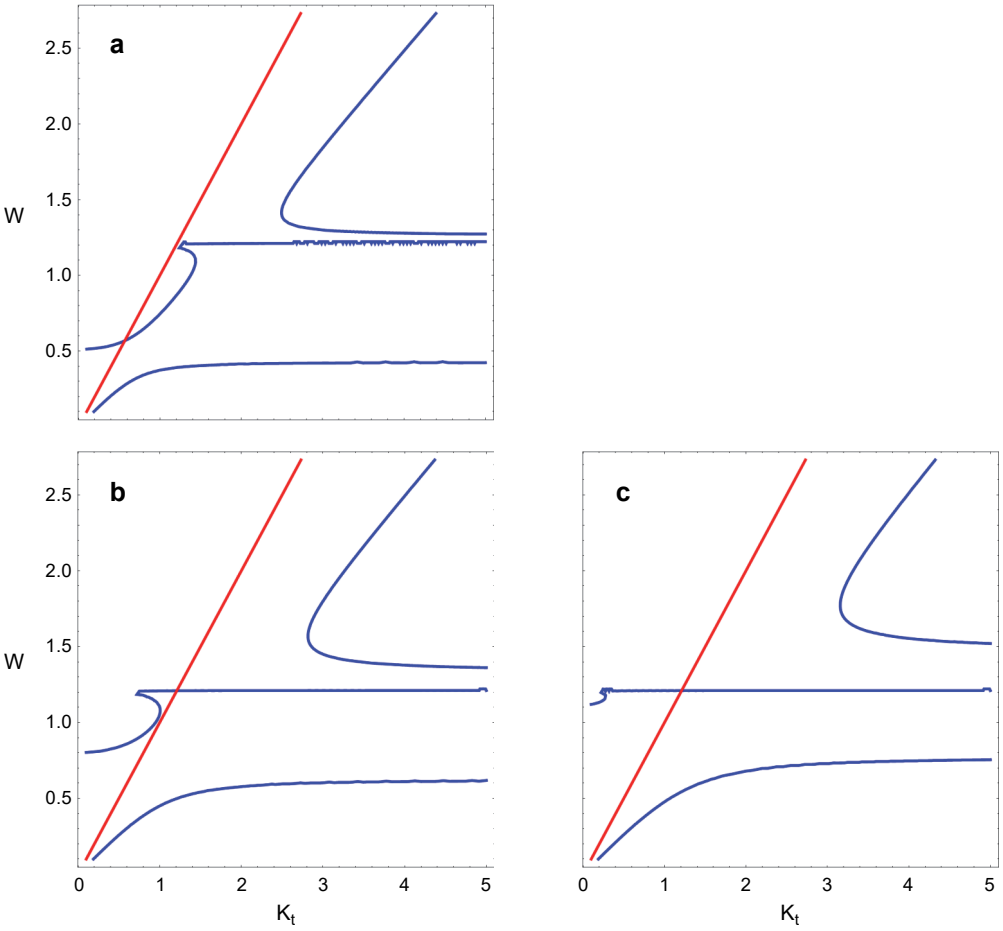

Fig. 4. The linear dispersion relation, *i.e*. the plots between W and K_t (blue curves) for different values of the filling factor $p = 0.2$ (**a**), $p = 0.4$ (**b**), and $p = 0.6$ (**c**). The red line is the light line.

of the parameter given in the figure captions. We explain the three curves one by one. Figure 4**a** is plotted for $p = 0.2$. The red line shows the light line. In the frequency region $W < 0.4$, where the metamaterial is behaving as type II hyperbolic metamaterial, there is the usual plasmon-polariton mode which lie away from the light line which means it cannot be directly excited by the external radiation. In the frequency region $0.4 < W < 1.0$, where the metamaterial is simple anisotropic, there is another mode which lies partially inside the light line indicating that it can directly be excited by the incident radiation in this region. It is interesting to note that in the region $1.0 < W < 1.2$, the part of the mode which lies outside the light line is left-handed ($dW/dK_x < 0$). In this frequency range, the metamaterial is type I hyperbolic metamaterial. For the frequency range $W > 1.2$, where the metamaterial is anisotropic, there is another mode outside

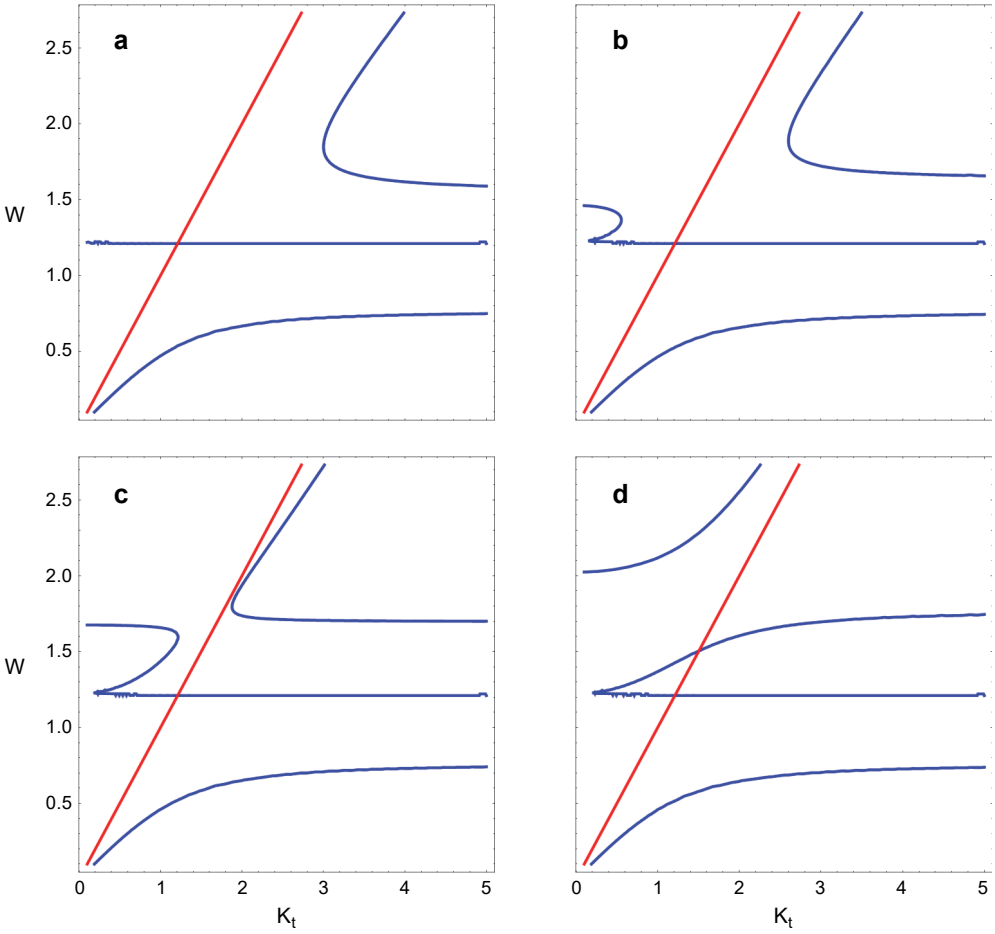

Fig. 5. The nonlinear dispersion relation, *i.e.* the plots between W and K_t (blue curves) corresponding to $p = 0.6$ for different values of the normalized incident intensity $I = 1.5$ (**a**), $I = 3$ (**b**), $I = 4$ (**c**), and $I = 5$ (**d**). The red line is the light line.

the light line which is partially left-handed ($dW/dK_x < 0$) and partially right-handed ($dW/dK_x > 0$). This mode is seen to move slightly towards the higher wave vector values as the filling factor increases in Fig. 4**b** ($p = 0.4$) and Fig. 4**c** ($p = 0.6$). Other modes also shift on the frequency region by changing the filling factor as the behavior of the metamaterial is affected as shown in Figs. 4**b** and 4**c**.

Next figures show the dispersion relations of the nonlinear surface waves. In Fig. 5, relation (21) has been plotted for different values of the normalized incident intensity ($I = |E_0|^2\alpha$) for a particular value of the filling factor ($p = 0.6$). If we compare Fig. 5**a** with Fig. 4**c** (showing dispersion relation of the linear surface waves for the same filling factor), it is clear that the lower plasmon-polariton mode lying in the frequency range $W > 0.7$, and the upper mode lying in the frequency range $W > 1.5$, are almost unaltered for this value of intensity ($I = 0.5$),whereas the intermediate mode has straightened to a line. When we move to a slightly higher value of intensity in Fig. 5**b**, we see that the nonlinearity has given birth to a new mode inside the light line which lies in the frequency region $1.2 < W < 1.5$. This mode is partially left-handed and partially right-handed. The upper mode has also shifted to the lower wave vector value. In Fig. 5**c** that has been plotted for a still higher value of intensity ($I = 4$), the intermediate mode expands on the frequency as well as on the wave vector scale whereas the upper mode shifts towards the lower value of the wave vector. The lower plasmon-polariton mode remains unaltered. In the last figure (Fig. 5**d**), we see that due to the higher value of intensity, the upper and the intermediate modes merge and give rise to two new modes. One lying in the frequency range $1.2 < W < 1.7$ which lies partially inside and partially outside the light line and is right-handed. The other lies completely inside the light line in the frequency range $W > 2.0$ and is right-handed. The lower surface plasmon-polariton mode remains unaltered by the incident intensity.

Lastly we consider the effect of material losses on the propagation length of the surface waves by drawing the figure of merit (FOM) curves of the lossy hyperbolic metamaterial. The figure of merit generally refers to the performance criteria of a given model and for the surface waves can be defined as $\mathrm{Re}(\varepsilon_\tau)/\mathrm{Im}(\varepsilon_\tau)$ at a given frequency for the lossy medium [41]. It is an indirect measure of the propagation length of the surface waves along the interface under consideration. In Fig. 6**a**, the FOM curves are plotted as a function of frequency for different values of the filling factor p. The figure shows that the value of FOM increases as the frequency increases for a given value of p. However, for a given value of frequency, the smaller the value of p, the higher is the value of FOM. This is quite obvious since smaller value of p refers to a smaller content of the lossy metal in the hyperbolic metamaterial. Another parameter that is used to consider the effect of the material losses is the dimensionless extinction coefficient defined as $\xi = \mathrm{Im}(k_\mathrm{n})d$, where k_n is the wave vector component perpendicular to the interface under consideration. The intensity of the surface waves inside the lossy metamaterial decreases proportional to $A(z) = \exp(-2z\xi/d)$. This parameter is an indirect measurement of the skin depth of the lossy hyperbolic metamaterial. In Fig. 6**b**, $A(z)$ is plotted as a function

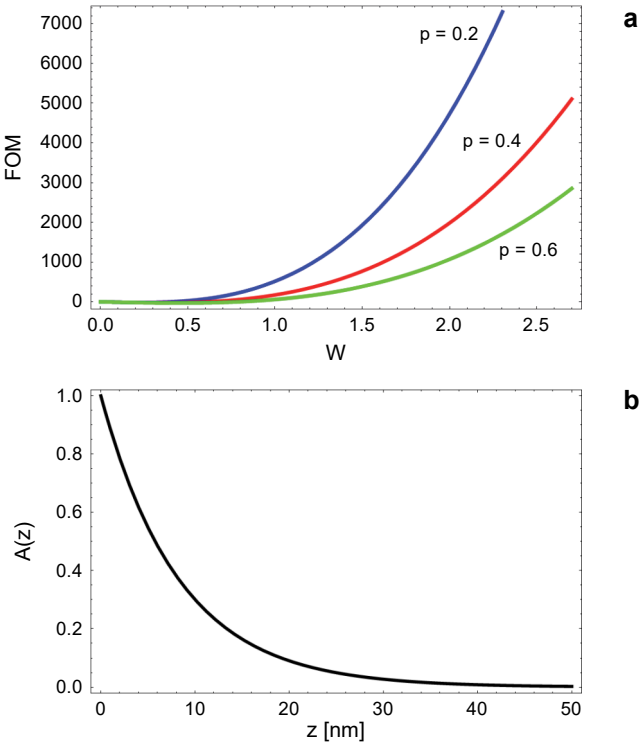

Fig. 6. The FOM curves corresponding to different values of the filling factor (**a**). The value of intensity $A(z)$ as a function of distance z in the lossy medium (**b**).

of z for $W = 2.0$. The figure shows that the intensity falls very rapidly perpendicular to the interface inside the lossy metamaterial indicating very well confined surface waves along the interface.

In conclusion, the linear and nonlinear TM surface waves at the interface between a dielectric material and an anisotropic metamaterial have been investigated. For the linear surface waves, the dispersion curves are plotted for different values of the filling factor. It is found that the change in filling factor affects the location of the modes on the frequency as well as on the wave vector axes. For the nonlinear surface waves, the intensity significantly affects the nature and location of the upper and the intermediate surface modes whereas the lower surface plasmon-polariton mode remains unaltered. So these linear and nonlinear surface waves can be engineered by the choice of the filling factor of the anisotropic metamaterial and the intensity of the incoming radiation. The effect of material losses is also considered by plotting the figure of merit and intensity profile curves perpendicular to the interface inside the lossy metamaterial. Lastly, it is important to mention that the calculations and results presented here are obtained under parallel uniaxial approximation for the permittivity tensor and are ap-

plicable for a particular choice of parameters. So in order to broaden the scale of the investigation, we hope to repeat the calculations under perpendicular uniaxial and isotropic approximation of the permittivity tensor.

References

[1] Cai W., Shalaev V.M., *Optical Metamaterials*, Springer, New York, NY, 2010.

[2] Shalaev V.M., *Optical negative refractive-index metamaterials*, Nature Photonics **1**, 2007, pp. 41–48, DOI: 10.1038/nphoton.2006.49.

[3] Zuojia Wang, Feng Cheng, Winsor T., Yongmin Liu, *Optical chiral metamaterials: a review of the fundamentals, fabrication methods and applications*, Nanotechnology **27**(41), 2016, article ID 412001, DOI: 10.1088/0957-4484/27/41/412001.

[4] Shekhar P., Atkinson J., Jacob Z., *Hyperbolic metamaterials: fundamentals and applications*, Nano Convergence **1**, 2014, article ID 14, DOI: 10.1186/s40580-014-0014-6.

[5] Xiujuan Zhang, Ying Wu, *Effective medium theory for anisotropic metamaterials*, Scientific Reports **5**, 2015, p. 7892, DOI: 10.1038/srep07892.

[6] Yuchu He, Eleftheriades G.V., *Anisotropic metamaterial as an antirefiection layer at extreme angles*, IEEE Transactions on Antennas and Propagation **65**(8), 2017, pp. 4102–4114, DOI: 10.1109/TAP.2017.2710213.

[7] Xiaoming Zhou, Gengkai Hu, *Superlensing effect of an anisotropic metamaterial slab with near-zero dynamic mass*, Applied Physics Letters **98**(26), 2011, article ID 263510, DOI: 10.1063/1.3607277.

[8] Zheping Shao, Yihao Yang, Zuojia Wang, Muhiddeen Yahaya, Bin Zheng, Shahram Dehdashti, Huaping Wang, Hongsheng Chen, *Manipulating surface plasmon polaritons with infinitely anisotropic metamaterials*, Optics Express **25**(9), 2017, pp. 10515–10526, DOI: 10.1364/OE.25.010515.

[9] Li G.X., Tam H.L., Wang F.Y., Cheah K.W., *Superlens from complementary anisotropic metamaterials*, Journal of Applied Physics **102**(11), 2007, article ID 116101, DOI: 10.1063/1.2817538.

[10] Fang A., Koschny T., Soukoulis C.M., *Optical anisotropic metamaterials: negative refraction and focusing*, Physical Review B **79**(24), 2009, article ID 245127, DOI: 10.1103/PhysRevB.79.245127.

[11] Pratap D., Ramakrishna S.A., Pollock J.G., Iyer A.K., *Anisotropic metamaterial optical fibers*, Optics Express **23**(7), 2015, pp. 9074–9085, DOI: 10.1364/OE.23.009074.

[12] Wei Xiang Jiang, Jessie Yao Chin, Tie Jun Cui, *Anisotropic metamaterial devices*, Materials Today **12**(12), 2009, pp. 26–33, DOI: 10.1016/S1369-7021(09)70314-1.

[13] Fernández-Núñez I., Bulashenko O., *Anisotropic metamaterial as an analogue of a black hole*, Physics Letters A **380**(1–2), 2016, pp. 1–8, DOI: 10.1016/j.physleta.2015.10.043.

[14] Othman M., Guclu C., Capolino F., *Graphene-dielectric composite metamaterials: evolution from elliptic to hyperbolic wavevector dispersion and the transverse epsilon- near-zero condition*, Journal of Nanophotonics **7**(1), 2013, article ID 073089, DOI: 10.1117/1.JNP.7.073089.

[15] Othman M.A.K., Guclu C., Capolino F., *Graphene-based tunable hyperbolic metamaterials and enhanced near-field absorption*, Optics Express **21**(6), 2013, pp. 7614–7632, DOI: 10.1364/OE.21.007614.

[16] Iorsh I.V., Mukhin I.S., Shadrivov I.V., Belov P.A., Kivshar Y.S., *Hyperbolic metamaterials based on multilayer graphene structures*, Physical Review B **87**(7), 2013, article ID 075416, DOI: 10.1103/PhysRevB.87.075416.

[17] García-Chocano V.M., Christensen J., Sánchez-Dehesa J., *Negative refraction and energy funneling by hyperbolic materials: an experimental demonstration in acoustics*, Physical Review Letters **112**(14), 2014, article ID 144301, DOI: 10.1103/PhysRevLett.112.144301.

[18] West P.R., Kinsey N., Ferrera M., Kildishev A.V., Shalaev V.M., Boltasseva A., *Adiabatically tapered hyperbolic metamaterials for dispersion control of high-k waves*, Nano Letters **15**(1), 2015, pp. 498–505, DOI: 10.1021/nl5038352.

[19] Smolyaninov I.I., *Holographic duality in nonlinear hyperbolic metamaterials*, Journal of Optics **16**(7), 2014, article ID 075101, DOI: 10.1088/2040-8978/16/7/075101.
[20] Ali M.Z., Bhatti A.A., Haque Q., Mahmood S., *Global transmission diagrams for evanescent waves in a nonlinear hyperbolic metamaterial*, Chinese Optics Letters **13**(9), 2015, article ID 090601.
[21] You-Chia Chang, Che-Hung Liu, Chang-Hua Liu, Siyuan Zhang, Marder S.R., Narimanov E.E., Zhaohui Zhong, Norris T.B., *Realization of mid-infrared graphene hyperbolic metamaterials*, Nature Communications **7**, 2016, article ID 10568, DOI: 10.1038/ncomms10568.
[22] Gric T., *Surface-plasmon-polaritons at the interface of vanostructured metamaterials*, Progress In Electromagnetics Research M **46**, 2016, pp. 165–172, DOI: 10.2528/PIERM15121605.
[23] Alshits V.I., Lyubimov V.N., *Dispersionless surface polaritons in the vicinity of different sections of optically uniaxial crystals*, Physics of the Solid State **44**(2), 2002, pp. 386–390, DOI: 10.1134/1.1451033.
[24] Eldlio M., Che F., Cada M., *Optical semiconductor surface-plasmon dispersion including losses using the Drude–Lorentz model*, Proceedings of the World Congress on Engineering and Computer Science 2012 Vol II WCECS 2012, October 24–26, 2012, San Francisco, USA.
[25] Dyakonov M.I., *New type of electromagnetic wave propagating at an interface*, Journal of Experimental and Theoretical Physics **67**(4), 1988, p. 714.
[26] Takayama O., Crasovan L.C., Johansen S.K., Mihalache D., Artigas D., Torner L., *Dyakonov surface waves: a review*, Electromagnetics **28**(3), 2008, pp. 126–145, DOI: 10.1080/02726340801921403.
[27] Mireta J.J., Sorní J.A., Naserpour M., Ardakani A.G., Zapata-Rodríguez C.J., *Nonlocal dispersion anomalies of Dyakonov-like surface waves at hyperbolic media interfaces*, Photonics and Nanostructures – Fundamentals and Applications **18**, 2016, pp. 16–22, DOI: 10.1016/j.photonics.2015.12.001.
[28] Zapata-Rodríguez C.J., Miret J.J., Vuković S., Belić M.R., *Engineered surface waves in hyperbolic metamaterials*, Optics Express **21**(16), 2013, pp. 19113–19127, DOI: 10.1364/OE.21.019113.
[29] Yuanjiang Xiang, Jun Guo, Xiaoyu Dai, Shuangchun Wen, Dingyuan Tang, *Engineered surface Bloch waves in graphene based hyperbolic metamaterials*, Optics Express **22**(3), 2014, pp. 3054–3062, DOI: 10.1364/OE.22.003054.
[30] Jacob Z., Narimanov E.E., *Optical hyperspace for plasmons: Dyakonov states in metamaterials*, Applied Physics Letters **93**(22), 2008, article ID 221109, DOI: 10.1063/1.3037208.
[31] Gric T., Cada M., Pistora J., *Propagation of surface waves formed at the interface between hyperbolic metamaterial and highly doped semiconductor*, Optical and Quantum Electronics **48**(4), 2016, article ID 237, DOI: 10.1007/s11082-016-0523-0.
[32] Takayama O., Shkondin E., Panah M.E.A., Repän T., Malureanu R., Jensen F., Lavrinenko A.V., *Surface waves on metal-dielectric metamaterials*, [In] *2016 18th International Conference on Transparent Optical Networks (ICTON)*, 2016, DOI: 10.1109/ICTON.2016.7550550.
[33] Ali M.Z., *Nonlinear surface waves in photonic hypercrystals*, Physics Letters A **381**(32), 2017, pp. 2643–2647, DOI: 10.1016/j.physleta.2017.05.060.
[34] Leung K.M., *Propagation of nonlinear surface polaritons*, Physical Review A **31**(2), 1985, p. 1189, DOI: 10.1103/PhysRevA.31.1189.
[35] Yu M.Y., *Surface polaritons in nonlinear media*, Physical Review A **28**(3), 1983, p. 1855, DOI: 10.1103/PhysRevA.28.1855.
[36] Langbein U., Lederer F., Mihalache D., Mazilu D., *Nonlinear TM-polarized waves in non-Kerr media*, Physica **145C**, 1987, p. 377.
[37] Boardman A.D., Maradudin A.A., Stegeman G.I., Twardowski T., Wright E.M., *Exact theory of nonlinear p-polarized optical waves*, Physical Review A **35**(3), 1987, p. 1159, DOI: 10.1103/PhysRevA.35.1159.
[38] Leung K.M., *p-polarized nonlinear surface polaritons in materials with intensity-dependent dielectric functions*, Physical Review B **32**(8), 1985, p. 5093, DOI: 10.1103/PhysRevB.32.5093.

[39] Stegeman G.I., Seaton C.T., Ariyasu J., Wallis R.F., Maradudin A.A., *Nonlinear electromagnetic waves guided by a single interface*, Journal of Applied Physics **58**(7), 1985, p. 2453, DOI: 10.1063/1.335920.

[40] Boyd R.W., Fischer G.L., *Nonlinear optical materials*, [In] *Encyclopedia of Materials: Science and Technology*, K.H.J. Buschow, R.W. Cahn, M.C. Flemings, B. Ilschner, E.J. Kramer, S. Mahajan, P. Veyssière [Eds.], 2001, pp. 6237–6244, DOI: 10.1016/B0-08-043152-6/01107-4.

[41] Narimanov E.E., *Photonic hypercrystals*, Physical Review X **4**(4), 2014, article ID 041014, DOI: 10.1103/PhysRevX.4.041014.

Received February 27, 2018
in revised form June 5, 2018